Exploring the effect of fractional degeneracy and the emergence of ray-wave duality in solid-state lasers with off-axis pumping

Y. F. Chen,* J. C. Tung, P. Y. Chiang, H. C. Liang, and K. F. Huang
Department of Electrophysics, National Chiao Tung University, 1001 Ta-Hsueh Road, Hsinchu 30050, Taiwan
(Received 10 May 2013; published 18 July 2013)

We employ the inhomogeneous Helmholtz equation to explore the influence of the fractional degeneracy and the pump distribution on the resonant lasing mode. Theoretical analyses clearly reveal the relationship between the fractional degeneracy and the emergence of the ray-wave duality. Furthermore, we perform thorough laser experiments to confirm the theoretical exploration that the resonant modes near the degenerate cavities are well localized on the ray trajectories under the condition of the off-axis pumping. We also exploit the derived wave functions to calculate the resonant strengths that can noticeably manifest the enhancements of the output powers in the degenerate cavities.

DOI: 10.1103/PhysRevA.88.013827 PACS number(s): 42.60.Da, 42.55.−f, 03.65.Sq, 73.23.−b

I. INTRODUCTION

Herriott *et al.* [1] in 1964 extended the analysis of paraxial electron beams [2] to show that an off-axis incident laser beam can be reflected in the two-mirror resonator forth and back to form a multipass ray orbit under the reentrant condition. To fulfill the reentrant condition, the cavity configuration requires satisfying the fractional degeneracy of $\Delta f_T/\Delta f_L = P/Q$, where P and Q are coprime integers, Δf_L is the longitudinal mode spacing, and Δf_T is the transverse mode spacing. The optical resonator satisfying the fractional degeneracy is usually called the degenerate cavity. In the early days, the Herriott-type multipass cavity has been used in diverse experiments, such as optical delay lines [3], absorption spectroscopy [4], Raman conversion [5–8], and high-power laser systems [9]. Recently, it has been experimentally found [10–17] that the lasing modes in off-axis pumped solid-state lasers have a preference to be localized on the periodic ray trajectories when the cavity lengths are somewhat close to the degenerate cavities. Furthermore, the variation of the output power with the cavity length was observed to exhibit significant fluctuations for the laser under the off-axis pumping. In particular, the output powers are found to be drastically increased in the vicinities of degenerate cavities [12,13]. Although several experimental data have been reported, so far there is no theoretical model to explore the effect of fractional degeneracy and the emergence of ray-wave duality near the degenerate cavities.

Over the past two decades, spatial structures of high-order modes generated from laser resonators have received much interest because of the similarity between Schrödinger and Helmholtz equations [18–21]. Numerous modern laser systems have been developed as analogous systems to visualize various quantum phenomena [22–25]. In mesoscopic quantum systems [26–32], the emergence of classical periodic orbits has been found to be tightly associated with the level degeneracy as well as the conductance fluctuation. Therefore, it is believed that exploring the emergence of ray-wave duality and the effect of fractional degeneracy in optical resonators can provide valuable insights, not only into laser physics but also into mesoscopic quantum phenomena.

In this work we originally exploit the inhomogeneous Helmholtz equation to perform a theoretical analysis for manifesting the influence of the fractional degeneracy and the pump distribution on the resonant lasing mode. Theoretical analyses and numerical calculations reveal that the lasing modes near the degenerate cavities turn out to be prominently localized on the ray trajectories under the condition of the off-axis pumping, especially for a large off-axis displacement. In experiments, we use a microchip laser with the off-axis pumping scheme to thoroughly measure the output power and the lasing pattern as a function of the cavity length for different off-axis displacements. Experimental results reveal that the emergence of the peaks in the output power variation with the cavity length is directly associated with the degenerate cavities. We further confirm that the spatial structures of the lasing modes near degenerate cavities can be excellently reconstructed with the theoretical resonant mode. Moreover, we employ the norm of the theoretical resonant mode to calculate the resonant strengths that are found to be in good agreement with the experimental results concerning the output power enhancements in the degenerate cavities.

Although the laser patterns in broad aperture lasers have been actively investigated for a long time, nearly all studies were mainly restricted to the single-longitudinal mode limit [33–36]. One special case is that the longitudinal-transverse mode degeneracy in the confocal cavity has been used as a trick to mimic the single-longitudinal mode situation to observe the transverse patterns and solitons experimentally [37,38]. It is believed that extending the studies to the general multilongitudinal mode case is an important step in light of pattern formation in broad aperture lasers.

II. THEORETICAL MODEL OF RESONANT LASING MODES

Without loss of generality, we consider a laser cavity forming by a gain medium, a concave spherical mirror, and a plane output coupler. For convenience, we use the effective optical length of the *ABCD* matrix to characterize the propagation property of the eigenmode inside the cavity.

*Corresponding author: Department of Electrophysics, National Chiao Tung University, 1001 TA Hsueh Road, Hsinchu 30010, Taiwan; yfchen@cc.nctu.edu.tw

The eigenmodes $\psi_{n,m,l}$ and the eigenvalues $k_{n,m,l}$ for a laser cavity can be solved from the Helmholtz equation:

$$\left(\nabla^2 + k_{n,m,l}^2\right)\psi_{n,m,l}(x,y,z) = 0, \tag{1}$$

Under the paraxial approximation, the eiegnmodes for the cavity with a concave mirror at $z = -L$ and a plane mirror at $z = 0$ can be expressed as the Hermite-Gaussian (HG) modes:

$$\psi_{n,m,l}^{(\mathrm{HG})}(x,y,z) = \sqrt{2/L}\,\Phi_{n,m}(x,y,z) \times \sin[k_{n,m,l}\tilde{z} - (m+n+1)\tan^{-1}(z/z_R)], \tag{2}$$

where

$$\Phi_{n,m}(x,y,z) = \frac{1}{\sqrt{2^{m+n-1}\pi m!n!}}\frac{1}{w(z)}H_n\left[\frac{\sqrt{2}x}{w(z)}\right]H_m\left[\frac{\sqrt{2}y}{w(z)}\right] \times \exp\left[-\frac{x^2+y^2}{w(z)^2}\right]. \tag{3}$$

$H_n(\bullet)$ is the Hermite polynomials of order n, $k_{n,m,l} = 2\pi f_{n,m,l}/c$, $f_{n,m,l}$ is the eigenmode frequency, $z_R = \sqrt{L(R-L)}$ is the Rayleigh range, R is the radius of curvature of the concave mirror, $\tilde{z} = z + [(x^2+y^2)z]/[2(z^2+z_R^2)]$, $w(z) = w_o\sqrt{1+(z/z_R)^2}$, $w_o = \sqrt{\lambda z_R/\pi}$ is the beam radius at the waist, and λ is the emission wavelength. The eigenmode frequency of the spherical cavity can be given by $f_{n,m,l} = [l\Delta f_L + (m+n+1)\Delta f_T]$, where l is the longitudinal mode index, and m and n are the transverse mode indices. For the concave-plano resonator, the transverse mode spacing Δf_T is given by $\Delta f_T = \Delta f_L[(1/\pi)\tan^{-1}(L/z_R)]$, where $\Delta f_L = c/2L'$, $L' = L + [n_c - (1/n_c)]L_c$, n_c is the refractive index of the gain medium, and L_c is the physical length of the gain medium. As a consequence, the mode-spacing ratio $\Omega = \Delta f_T/\Delta f_L = [(1/\pi)\tan^{-1}(L/z_R)]$ for a given value of R can be varied in the range between 0 and 1/2 by changing the cavity length within $0 < L < R$. The spectrum $f_{n,m,l}$ for a given R can be calculated as a function of the cavity length L. Figure 1(a) depicts a portion of the calculated results for the spectrum $f_{n,m,l}/\Delta f_L$ versus the ratio L/R in the range of $5 \leqslant l \leqslant 15$ and $0 \leqslant (m+n) \leqslant 10$, where $L = L'$ is used for convenience. It can be seen that the relative spectrum $f_{n,m,l}/\Delta f_L$ versus the ratio L/R displays numerous degeneracies and frequency gaps at the cavity lengths corresponding to the degenerate cavities with $\Omega = [(1/\pi)\tan^{-1}(L/z_R)] = P/Q$. In terms of the degenerate conditions of $\Omega = P/Q$, the relative spectrum can be expressed as $f_{n,m,l}/\Delta f_L = N/Q$ with $N = [lQ + (m+n+1)P]$. For a given set of (P, Q), it follows that the frequency levels are degenerate because there may be many combinations of (n, m, l) satisfying the equation $N = [lQ + (m+n+1)P]$, resulting in frequency gaps in the spectrum $f_{n,m,l}/\Delta f_L$ as N changes by unity. The accidental degeneracy in the quantum spectra has been discussed to play a crucial role in the relationship between quantum shell structures and classical periodic orbits, especially in the mesoscopic systems [27–32]. In the optical cavity, the occurrence of the mode degeneracy can also be linked to the appearance of the periodic ray paths. Figures 1(b) and 1(c) show the periodic ray paths for the cases of $\Omega = 1/3$ and $\Omega = 6/19$, respectively. In contrast, when Ω is not rational, the path never closes and fills the space, as shown in Fig. 1(d).

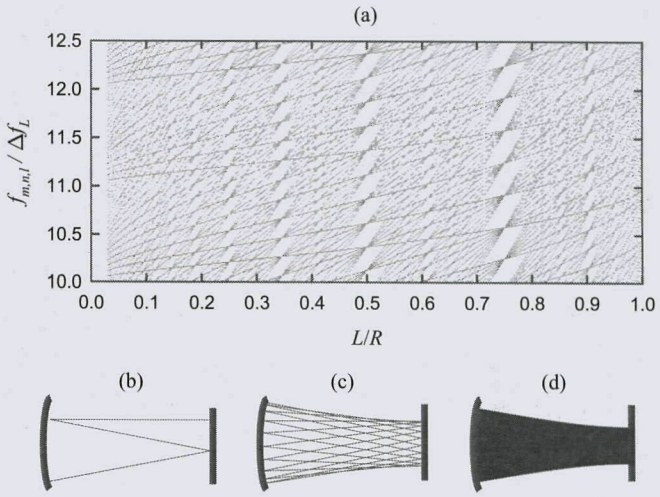

FIG. 1. (Color online) (a) A portion of the spectrum $\Delta f_{n,m,l}/\Delta_L$ as a function of the ratio L/R for the range of $5 \leqslant l \leqslant 15$ and $0 \leqslant (m+n) \leqslant 10$. (b), (c) Periodic ray paths for the cases of $\Omega = 1/3$ and $\Omega = 6/19$, respectively. (d) A case of the path for Ω to be not rational.

As found in much of the literature [10–17], the lasing modes in an off-axis pumping resonator are not always the high-order HG modes; in particular, the lasing modes are usually found to be concentrated on the ray trajectories in the degenerate cavity. In principle, the resonant modes of the laser system pumped by a localized source can be solved from the inhomogeneous Helmholtz equation. While the inhomogeneous Helmholtz equation is frequently used to analyze the free-space propagation of the time-harmonic wave in electrodynamics, we exploit this type of equation to analyze the resonant lasing modes in the locally pumped laser systems. Considering the pump source distribution $F(x,y,z)$, the inhomogeneous Helmholtz equation for deriving the resonant modes is given by

$$(\nabla^2 + \tilde{k}^2)\Psi(x,y,z) = \eta_c F(x,y,z), \tag{4}$$

where $\tilde{k} = k + i\alpha$, $k = 2\pi/\lambda$ is the wave number of the emission light, the factor η_c represents the conversion efficiency for the excitation source, and α is a small loss parameter including losses from the scattering, the absorption, and the output coupling. The resonant lasing modes are basically subject to the same boundary condition as the homogeneous Helmholtz in Eq. (1) for HG eigenmodes. With the expansion of eigenmodes, the lasing mode and the source distribution can be expressed as the superposition of HG eigenmodes:

$$\Psi(x,y,z) = \sum_{n,m,l} a_{n,m,l}\psi_{n,m,l}^{(\mathrm{HG})}(x,y,z) \tag{5}$$

and

$$\eta_c F(x,y,z) = \sum_{n,m,l} b_{n,m,l}\psi_{n,m,l}^{(\mathrm{HG})}(x,y,z). \tag{6}$$

Substituting into the wave equation (4), the relationship between the coefficients $a_{n,m,l}$ and $b_{n,m,l}$ can be found to be $a_{n,m,l} = b_{n,m,l}/(\tilde{k}^2 - k_{n,m,l}^2)$. Considering the condition of $\alpha \ll k$, the eigenmode expansion of the resonant mode can be

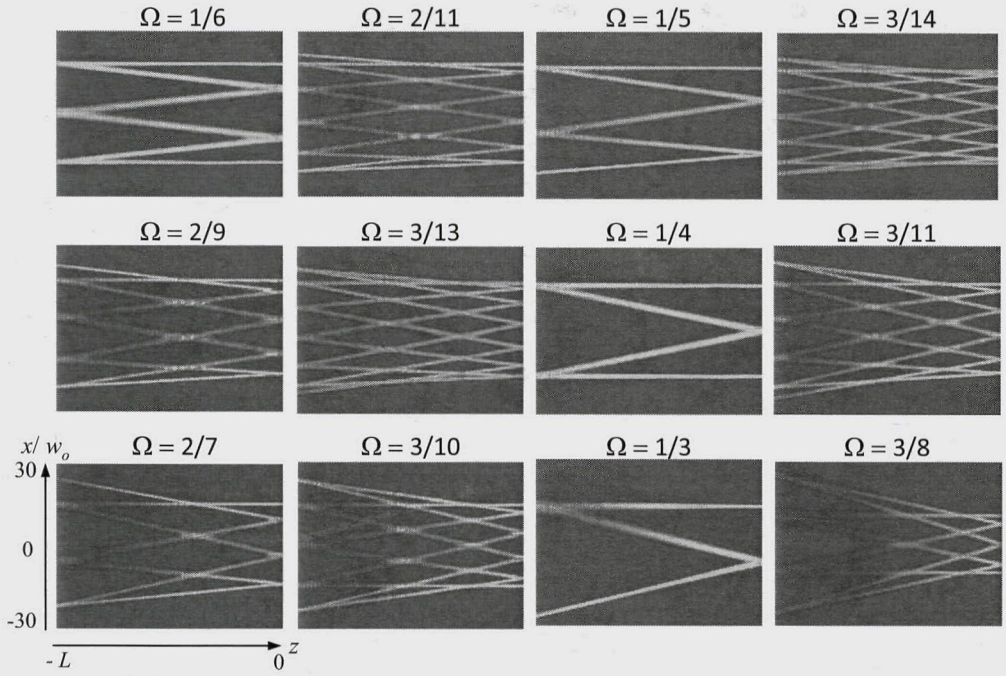

FIG. 2. (Color online) Calculated wave patterns $|\Psi(x,y,z)|^2$ inside the laser cavities for various rational numbers of the mode-spacing ratio Ω.

given by

$$\Psi(x,y,z) = \sum_{n,m,l} \frac{b_{n,m,l}}{(k^2 - k_{n,m,l}^2) + 2i\alpha k} \psi_{n,m,l}^{(\mathrm{HG})}(x,y,z). \quad (7)$$

With the orthonormal property of eigenmodes, the coefficient $b_{n,m,l}$ is given by

$$b_{n,m,l} = \eta_c \iiint \psi_{n,m,l}^{(\mathrm{HG})}(x,y,z) F(x,y,z) dx dy dz. \quad (8)$$

In general, the distribution of the pump source $F(x,y,z)$ in the longitudinal z direction can be approximated to be uniform. On the other hand, the transverse distribution of the pump source $F(x,y,z)$ is similar to a Gaussian distribution. Consequently, the pump source $F(x,y,z)$ for the off-axis pumping with a transverse displacement Δx in the x direction can be given by

$$F(x,y,z) = \frac{2}{\pi w^2(z) L_c} \exp\left[-\frac{(x-\Delta x)^2 + y^2}{w^2(z)}\right], \quad (9)$$

for $|z - z_c| \leqslant L_c/2$, where z_c is the location of the gain medium. Since the longitudinal distribution of the pump source is nearly uniform, the coefficient $b_{n,m,l}$ related to the source term $F(x,y,z)$ can be considered to be independent of the index l in the neighborhood of the central index l_o. Consequently, the integral for determining the coefficient $b_{n,m,l}$ can be approximately reduced as

$$b_{n,m,l} = \frac{\eta}{L_c} \frac{2}{\pi w^2(z_c)} \iint \Phi_{n,m}^{(\mathrm{HG})}(x,y,z_c) \times \exp\left[-\frac{(x-\Delta x)^2 + y^2}{w^2(z_c)}\right] dx dy, \quad (10)$$

where η is a constant that includes the effective conversion efficiency η_c and the overlap integral in the longitudinal direction. Substituting Eqs. (3) and (9) into Eq. (10) and using the generating function of the Hermite polynomials, the coefficient $b_{n,m,l}$ can be evaluated to be

$$b_{n,m,l} = \frac{\eta}{L_c} \sqrt{\frac{2}{\pi w^2(z_c)}} \left[\frac{(n_o)^{n/2}}{\sqrt{n!}} e^{-n_o/2}\right] \delta_{m,0}, \quad (11)$$

where $n_o = [\Delta x / w(z_c)]^2$. Note that the value of the parameter n_o signifies the magnitude of the off-axis displacement. Equation (11) also indicates that the maximum contribution in the resonant mode comes from the eigenmode with the transverse index n to be closest to the value n_o. For convenience, we take the parameter n_o to be the integer closest to the value of $[\Delta x / w(z_c)]^2$. Moreover, the expression in the square bracket of Eq. (11) is just the form of the square root of the Poisson distribution. With the central limit theorem, the Poisson distribution approaches the Gaussian distribution for large value of n_o. Equation (11) can therefore be expressed as [39]

$$b_{n,m,l} = \frac{\eta}{L_c} \sqrt{\frac{2}{\pi w^2(z_c)}} \frac{1}{\sqrt{\sqrt{2\pi n_o}}} \exp\left[-\frac{(n-n_o)^2}{4n_o}\right] \delta_{m,0}. \quad (12)$$

Equation (12) clearly indicates that the maximum amplitude for the coefficient $b_{n,m,l}$ occurs at the indices of $n = n_o$ and $m = 0$. With the property of the Gaussian distribution, the effective range of mode index n can be limited as $|n - n_o| \leqslant N$ with $N = 2\sqrt{n_o}$. For a given wave number k, the longitudinal index of the central eigenmode in the resonant mode can be determined from the expression of $k = \pi[l_o + (n_o + 1)\Omega]/L'$. Substituting Eq. (12) into Eq. (7) and in terms of n_o and l_o,

the resonant mode can be further derived as

$$\Psi(x,y,z) = \frac{\eta\lambda L'}{4\pi^2 L_c}\sqrt{\frac{2}{\pi w^2(z_c)}}\frac{1}{\sqrt{\sqrt{2\pi n_o}}}\left\{\sum_{l=l_o-J}^{l_o+J}\sum_{n=n_o-N}^{n_o+N}\frac{\exp[-(n-n_o)^2/4n_o]}{[(l_o-l)+(n_o-n)\Omega]+i\gamma}\psi^{(\mathrm{HG})}_{n,m,l}(x,y,z)\right\}, \tag{13}$$

where J is related to the effective range of mode index l and $\gamma = \alpha L'/\pi$ represents the inverse quality factor. The denominator in the coefficient of Eq. (13) indicates that only the degenerate and nearly degenerate eigenmodes play the main role in the formation of the resonant mode. The nearly degenerate requirement leads to the value of J to be the integer closest to $N\Omega$.

For given values of the parameters n_o, k, α, and R, the resonant mode $\Psi(x,y,z)$ can be calculated with Eq. (13) as a function of the ratio Ω. Here we use the parameters of a typical Nd-doped solid-state laser with $R = 30$ mm, $\alpha = 10^{-3}$ mm, and $\lambda = 1064$ nm to calculate the resonant patterns $|\Psi(x,y,z)|^2$ for various degenerate cavities. The values of the parameter n_o used in the calculation are in the range of 120–330 for different Ω values. The calculated patterns $|\Psi(x,y,z)|^2$ are shown in Fig. 2 for several rational numbers of the mode-spacing ratio Ω. It can be seen that the wave patterns $|\Psi(x,y,z)|^2$ are excellently localized on the ray trajectories. The promising manifestation of the ray-wave duality not only confirms the significance of the wave function in Eq. (13) but also validates the analysis with the inhomogeneous Helmholtz equation in Eq. (4).

Since $|a_{n,m,l}|^2$ is the relative probability of the resonant mode $\Psi(x,y,z)$ in the eigenstate $\psi^{(\mathrm{HG})}_{n,m,l}(x,y,z)$, we use the total summation $\sum_{n,m,l}|a_{n,m,l}|^2$ to evaluate the resonant strength. With Eq. (13), the resonant strength can be expressed as

$$I(\Delta x, L) = \left(\frac{\eta\lambda L'}{4\pi^2 L_c}\right)^2 \frac{2}{\pi w^2(z_c)}\frac{1}{\sqrt{2\pi n_o}} \times \sum_{l=l_o-J}^{l_o+J}\sum_{n=n_o-N}^{n_o+N}\frac{\exp[-(n-n_o)^2/2n_o]}{[(l_o-l)+(n_o-n)\Omega]^2+\gamma^2}. \tag{14}$$

In the conventional theory, the output power is proportional to the overlap efficiency between the pump region and the lasing mode. In the present theory, the overlap integral is associated with the coefficient $b_{n,m,l}$ in Eq. (8). The factor $(\tilde{k}^2 - k^2_{n,m,l})$ in the expression of $a_{n,m,l} = b_{n,m,l}/(\tilde{k}^2 - k^2_{n,m,l})$ determines the cavity modes that can effectively participate in the laser radiation. To be brief, Eq. (14) not only includes the overlap efficiency but also considers the influence of the efficient number of participating modes on the laser emission. In the following, we employ an off-axis end-pumped microchip laser to systematically verify the present theoretical analysis by means of measuring the lasing mode and the output power under the variation of the cavity length.

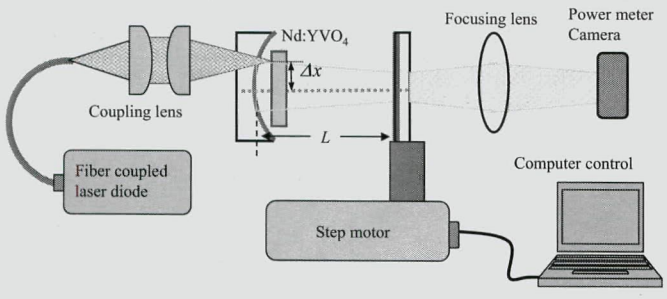

FIG. 3. (Color online) Experimental setup for measuring the dependence of the output power variation and the lasing patterns on the cavity length in a concave-plano resonator with several off-axis displacements.

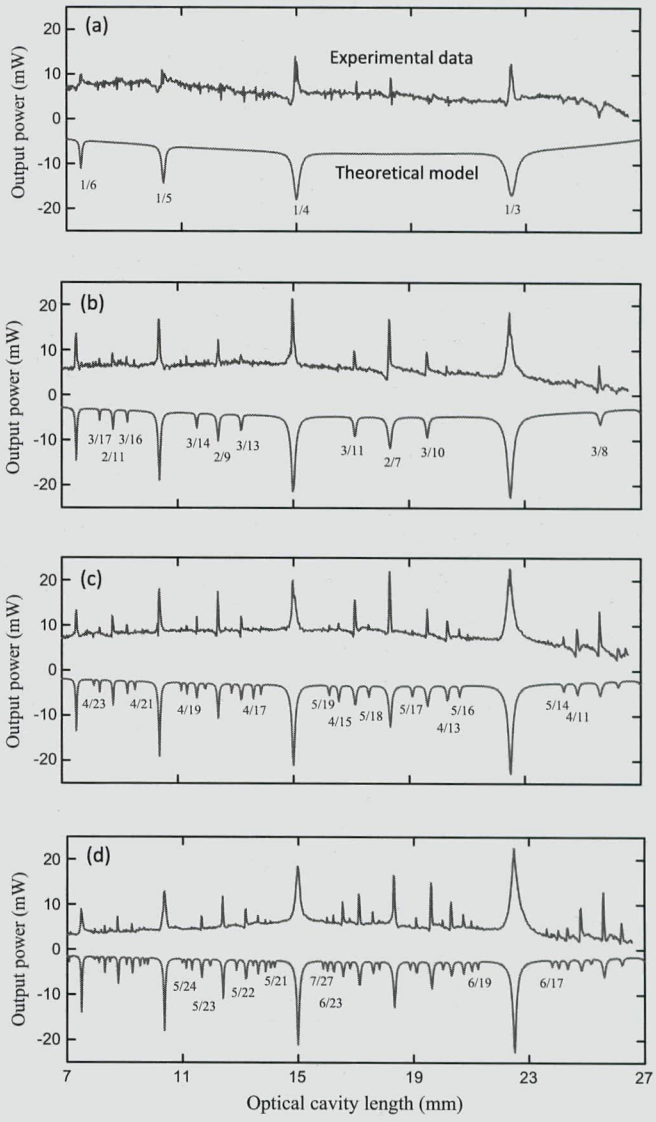

FIG. 4. (Color online) (a)–(d) Dependence of the output power variation on the cavity length for the off-axis displacements of 0.5, 1.0, 1.5, and 2.0 mm, respectively. The experimental and theoretical results are displayed as mirror images.

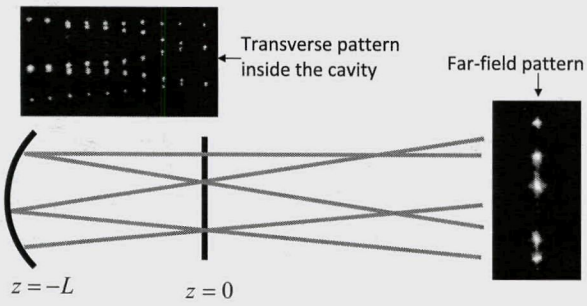

FIG. 5. (Color online) Measured transverse patterns inside the cavity and the experimental far-field pattern for the cavity length near $\Omega = 1/5$.

III. EXPERIMENTAL VERIFICATION

In contemporary solid-state lasers, the off-axis pumping scheme has been confirmed to be a promising method for the production and manipulation of various transverse modes from fundamental state to super high-order states [10–17]. Figure 3 depicts the experimental setup for exploring the dependence of the output power variation on the cavity length in a concave-plano resonator with several off-axis displacements. The laser medium was an a-cut 2.0-at.% Nd^{3+}:YVO4 crystal with a length of 2 mm. Both sides of the Nd:YVO4 crystal were coated for antireflection at 1064 nm (reflection <0.1%). The gain medium was quite close to the concave mirror with a separation of nearly 1 mm. The radius of curvature of the concave mirror is $R = 30$ mm and the reflectivity is 99.8% at 1064 nm. The output coupler is a flat mirror with a transmission of 2% at 1064 nm. The output coupler was mounted on a translation stage driven with a step motor to precisely control the cavity length in the range of 7–27 mm. The pump source was an 809-nm fiber-coupled laser diode with a core diameter of 100 μm, a numerical aperture of 0.16, and a maximum output power of 3 W. A focusing lens with a 20-mm focal length and 90% coupling efficiency was used to reimage the pump beam into the laser crystal. The pump radius was estimated to be approximately 25 μm. The off-axis displacement Δx could be varied in the range of 0–2.5 mm. The output power was measured with the synchronization of the variation of the cavity length under the control of a microcomputer.

At a pump power of 1.5 W, the emission powers were found to be on the order of 10 mW. Figures 4(a)–4(d) show the experimental results for the variation of the output power with

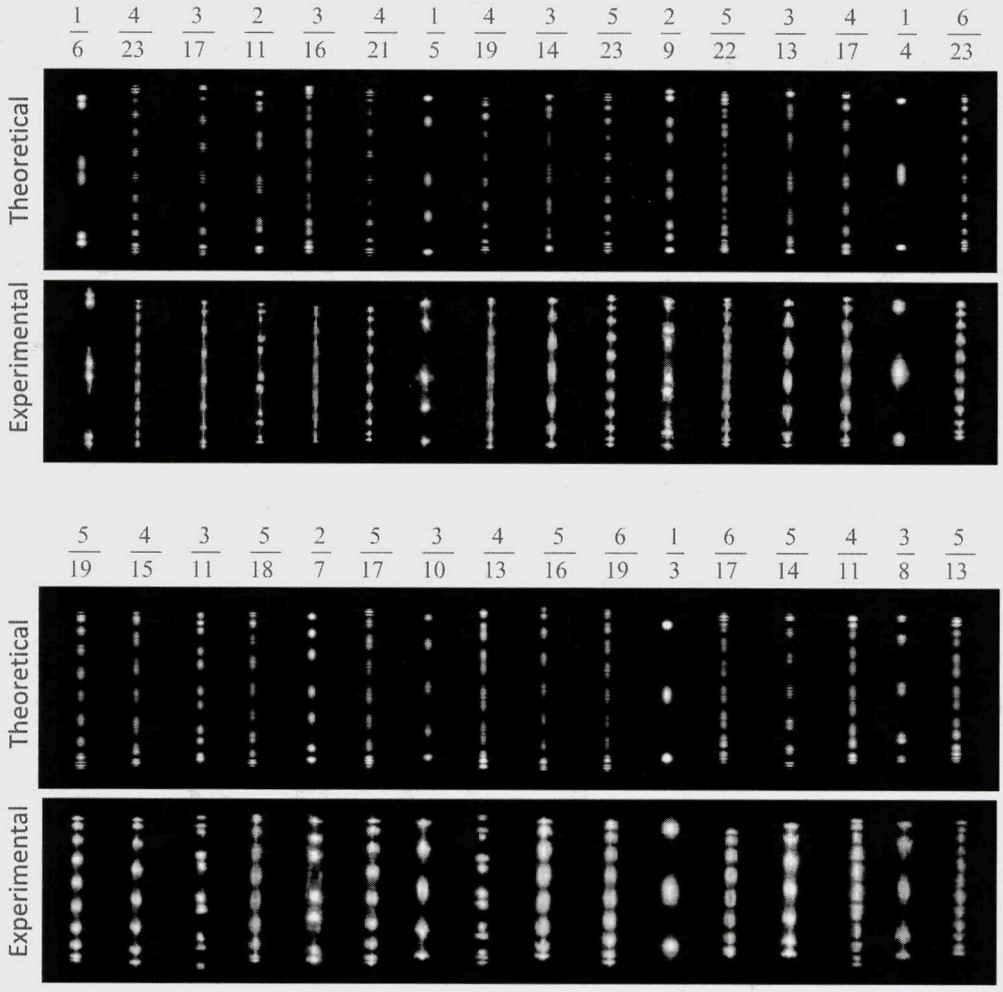

FIG. 6. (Color online) A series of experimental far-field patterns measured at the position of $z = 20$ cm for the different denigrate cavities. Corresponding to experimental results, theoretical patterns are calculated with Eq. (13) and shown for comparison.

the cavity length at four different off-axis displacements of 0.5, 1.0, 1.5, and 2.0 mm. The theoretical results corresponding to the experimental observations were calculated with Eq. (14) and the parameters of $R = 30$ mm, $\alpha = 10^{-3}$ mm, and $\lambda = 1064$ nm. For comparison, the theoretical results are also shown in Figs. 4(a)–4(d) with mirror images to the experimental observations. The scaling factor for the height of the calculated resonance strength is adjusted with the best fit to the experimental data. It can be found that the experimental output power variations agree very well with the relative values of the resonance strength. As shown in Figs. 4(a)–4(d), the enhancements of the output powers are in good agreement with the appearances of the fractional degeneracies in which the mode-spacing ratio Ω corresponds to a rational number P/Q. It is also clear that the larger the off-axis displacement Δx is given, the more resonance peaks appear in the output power variation on the cavity length. Since a larger off-axis displacement leads to the generation of higher-order transverse modes, it can be confirmed that the influence of the fractional degeneracy on the output power enhancement significantly increases with increasing the transverse order. In other words, the generation of higher-order transverse modes plays an important role in manifesting the lasing mode localized on a more complicated periodic orbit. Increasing the pump power by several times above threshold, the overall feature of the enhancing part remains but the smoothly varying part becomes higher.

To further verify the relationship between the fractional degeneracy and the periodic ray trajectory, the lasing patterns for each resonant peak in the output power variation were recorded. We use the lens to reimage the transverse patterns at the different longitudinal positions inside the cavity. Figure 5 shows the measured transverse patterns for the cavity length near $\Omega = 1/5$. The experimental patterns can be seen to be well localized on the ray trajectories. Besides, the far-field pattern shown in Fig. 5 clearly displays a characteristic of multiple spots. Figure 6 shows a series of experimental far-field patterns measured at the position of $z = 20$ cm for the different cavity lengths that specifically correspond to the peaks of the output power variation shown in Fig. 4. Theoretical far-field patterns calculated with Eq. (13) are also shown in Fig. 6 for comparison. The good agreement between experimental results and theoretical patterns not only confirms the physical analysis but also validates the present theoretical model. This use of the inhomogeneous Helmholtz equation explains the appearance of the resonant modes localized on the ray trajectories in laser systems.

IV. CONCLUSIONS

In summary, we have theoretically used the inhomogeneous Helmholtz equation to explore the influence of the fractional degeneracy and the pump distribution on the resonant lasing mode. Theoretical analyses manifest that the fractional degeneracy leads to the lasing modes to be well localized on the ray trajectories under the condition of the off-axis pumping, especially for a large off-axis displacement. For verifying the theoretical exploration, we have employed a microchip laser with the off-axis pumping scheme to measure the output power and the lasing pattern as a function of the cavity length for different off-axis displacements. Experimental results confirm that the emergence of the lasing modes with ray-wave duality is directly associated with the degenerate cavities. We have also verified that the transverse patterns of the lasing modes near degenerate cavities can be remarkably reconstructed with the theoretical model. Finally, the experimental results concerning the output power enhancements in the degenerate cavities are also well manifested with the resonant strengths calculated with the theoretical resonant modes.

ACKNOWLEDGMENTS

This work is supported by the National Science Council of Taiwan (Contract No. NSC-100-2628-M-009-001-MY3).

[1] D. R. Herriott, H. Kogelnik, and R. Kompfner, Appl. Opt. **3**, 523 (1964).
[2] J. R. Pierce, *Theory and Design of Electron Beams* (Van Nostrand, New York, 1954), pp. 194–197.
[3] D. R. Herriott and H. J. Schulte, Appl. Opt. **4**, 883 (1965).
[4] A. Owyoung, C. W. Patterson, and R. S. Mcdowell, Chem. Phys. Lett. **59**, 156 (1978).
[5] R. L. Byer and W. R. Trutna, Opt. Lett. **3**, 144 (1978).
[6] P. Rabinowitz, A. Stein, R. Brickman, and A. Kaldor, Opt. Lett. **3**, 147 (1978).
[7] K. Midorikawa, H. Tashiro, Y. Aoki, K. Nagasaka, K. Toyoda, and S. Namba, Appl. Phys. Lett. **47**, 1033 (1985).
[8] W. R. Trutna and R. L. Byer, Appl. Opt. **19**, 301 (1980).
[9] J. G. Xin, A. Duncan, and D. R. Hall, Appl. Opt. **28**, 4576 (1989).
[10] T. Brand, B. Ozygus, and H. Weber, Laser Phys. **8**, 1 (1998).
[11] J. Erhard, H. Laabs, B. Ozygus, H. Weber, and Q. Zhang, Proc. SPIE **3611**, 2 (1999).
[12] Q. Zhang, B. Ozygus and H. Weber, Eur. Phys. J.: Appl. Phys. **6**, 293 (1999).
[13] J. Dingjan, M. P. van Exter, and J. P. Woerdman, Opt. Commun. **188**, 345 (2001).
[14] H. H. Wu and W. F. Hsieh, J. Opt. Soc. Am. B **18**, 7 (2001).
[15] Y. F. Chen, C. H. Jiang, Y. P. Lan, and K. F. Huang, Phys. Rev. A **69**, 053807 (2004).
[16] A. A. Malyutin, Quantum Electron. **37**, 299 (2007).
[17] A. A. Malyutin, Quantum Electron. **38**, 181 (2008).
[18] Y. F. Chen and Y. P. Lan, Phys. Rev. A **65**, 013802 (2001).
[19] K. F. Huang, Y. F. Chen, H. C. Lai, and Y. P. Lan, Phys. Rev. Lett. **89**, 224102 (2002).
[20] T. Gensty, K. Becker, I. Fischer, W. Elsäßer, C. Degen, P. Debernardi, and G. P. Bava, Phys. Rev. Lett. **94**, 233901 (2005).
[21] Y. F. Chen, T. H. Lu, K. W. Su, and K. F. Huang, Phys. Rev. Lett. **96**, 213902 (2006).
[22] E. J. Galvez, P. R. Crawford, H. I. Sztul, M. J. Pysher, P. J. Haglin, and R. E. Williams, Phys. Rev. Lett. **90**, 203901 (2003).
[23] I. Vorobeichik, E. Narevicius, G. Rosenblum, M. Orenstein, and N. Moiseyev, Phys. Rev. Lett. **90**, 176806 (2003).

[24] Y. F. Chen, K. W. Su, T. H. Lu, and K. F. Huang, Phys. Rev. Lett. **96**, 033905 (2006).
[25] C. C. Chen, Y. T. Yu, Ross C. C. Chen, Y. J. Huang, K. W. Su, Y. F. Chen, and K. F. Huang, Phys. Rev. Lett. **102**, 044101 (2009).
[26] C. M. Marcus, A. J. Rimberg, R. M. Westervelt, P. F. Hopkins, and A. C. Gossard, Phys. Rev. Lett. **69**, 506 (1992).
[27] J. P. Bird, D. K. Ferry, R. Akis, Y. Ochiai, K. Ishibashi, Y. Aoyagi, and T. Sugano, Europhys. Lett. **35**, 529 (1996).
[28] S. M. Reimann, M. Persson, P. E. Lindelof, and M. Brack, Z. Phys. B **101**, 377 (1996).
[29] I. V. Zozoulenko, R. Schuster, K. F. Berggren, and K. Ensslin, Phys. Rev. B **55**, R10209 (1997).
[30] L. Christensson, H. Linke, P. Omling, P. E. Lindelof, I. V. Zozoulenko, and K.-F. Berggren, Phys. Rev. B **57**, 12306 (1998).
[31] B. L. Johnson and G. Kirczenow, Europhys. Lett. **51**, 367 (2000).
[32] M. Brack, Rev. Mod. Phys. **65**, 677 (1993).
[33] K. Staliunas and V. J. Sanchez-Morcillo, *Transverse Patterns in Nonlinear Optical Resonators*, Spinger Tracts in Modern Physics Vol. 183 (Spinger Verlag, Berlin, 2003).
[34] M. Brambilla, F. Battipede, L. A. Lugiato, V. Penna, F. Prati, C. Tamm, and C. O. Weiss, Phys. Rev. A **43**, 5090 (1991).
[35] D. Dangoisse, D. Hennequin, C. Lepers, E. Louvergneaux, and P. Glorieux, Phys. Rev. A **46**, 5955 (1992).
[36] E. Louvergneaux, D. Hennequin, D. Dangoisse, and P. Glorieux, Phys. Rev. A **53**, 4435 (1996).
[37] K. Staliunas, G. Slekys, and C. O. Weiss, Phys. Rev. Lett. **79**, 2658 (1997).
[38] V. B. Taranenko, K. Staliunas, and C. O. Weiss, Phys. Rev. Lett. **81**, 2236 (1998).
[39] Y. F. Chen, Phys. Rev. A **83**, 032124 (2011).